# Molecular dynamics study of size effects in the compression of metallic glass nanowires

Francesco Delogu*
*Dipartimento di Ingegneria Chimica e Materiali, Università degli Studi di Cagliari, piazza d'Armi, 09123 Cagliari, Italy*
(Received 16 December 2008; revised manuscript received 24 February 2009; published 15 May 2009)

Molecular dynamics simulations have been employed to investigate the mechanical response to uniaxial compression of metallic glass nanowires with radius in the range between 1 and 6 nm. It is found that the mechanical behavior of nanowires, based on the activity of shear transformation zones, is affected by size effects. The nanowires in which the largest number of shear transformation zones involve only bulk atoms exhibit a behavior similar to that of bulk systems. When a relatively large number of shear transformation zones can also involve surface atoms, the mechanical response of the nanowire changes. It seems in particular that atomic volume effects determine the loss of correlation between consecutive atomic rearrangements. As a consequence, shear transformation zones are no longer able to exhibit an autocatalytic dynamics. The mechanical response of the nanowires with smallest radii is correspondingly different from the one of other nanowires.

DOI: 10.1103/PhysRevB.79.184109 PACS number(s): 61.46.Df, 61.43.Fs

## I. INTRODUCTION

Metallic glasses (MGs) are currently the focus of intense studies in view of their possible application as structural materials.[1,2] Most of these studies are aimed at characterizing, understanding, and possibly controlling the atomistic mechanisms responsible for the limited ductility of MGs at room temperature.[1,2] It is in fact precisely this feature to prevent their practical use despite the suite of highly desirable mechanical properties possessed, i.e., elastic moduli on the same order of magnitude than conventional engineering materials but considerably larger strength at room temperature.[1,2] Such undesired behavior can be ascribed to the absence of long-range structural order, which does not permit the formation of dislocations, the most important plasticity carriers in crystalline systems.[1,2] MG deformation, thus, occurs via the operation of flow defects generally referred to as shear transformation zones (STZs).[3–7] Homogeneously distributed within the glassy structure, these are formed by groups of roughly 10 to 100 atoms undergoing a local rearrangement from a relatively low-energy configuration to a similar one across a relatively high activation barrier.[3–7] Rearrangements, thought to operate when local atomic strains exceed a certain critical threshold,[3–7] exhibit a strong autocatalytic behavior and are responsible for a considerable flow softening.[8–16] As a consequence, plastic deformation often suffers of a severe instability that determines the localization of strains in so-called shear bands (SBs) about 10 to 20 nm thick.[8–16] Once generated, SBs can quickly evolve into cracks and the MGs undergo a failure process typical of macroscopically brittle materials.[8–16]

The limited SB thickness poses fundamental questions about the nature of STZ interaction processes when the number of STZs is intrinsically limited by the volume of the MG system undergoing deformation. It is indeed reasonable to expect that SB nucleation processes could significantly change, and even be suppressed, when the MG volume reduces to the nanometer scale.[2] A few evidences of the change of MG deformation mechanisms with the system size have been recently obtained,[17–20] which indicate that deformation is no longer as inhomogeneous as in macroscopic MG samples. This suggests that nanometer-sized systems could exhibit relatively large plasticity and that the knowledge of atomic-scale mechanisms involved in their deformation behavior could be exploited to improve the mechanical properties of massive MGs.[2,20]

Along this line, the present work represents an attempt to provide further information on the deformation behavior of nanometer-sized MGs by taking advantage of molecular dynamics (MD) simulations. To such aim, a binary $Ni_{50}Zr_{50}$ metallic glass has been selected as model system. Calculations have been performed on cylindrical nanowires (NWs) with radius ranging between 1 and 6 nm subjected to uniaxial compression under displacement-controlled conditions. Analyses have been focused on the very initial stages of deformation. Details of MD methods are given in the following. Before discussing them, it is however worth noting that a few questions representing the fundamental motivations for the present work originate from a previous study on the mechanical behavior of a roughly spherical nanometer-sized particle of $Ni_{50}Zr_{50}$ alloy with amorphous structure.[21]

Such numerical study pointed out significant differences between rearrangements involving only bulklike or also surface ones.[21] More specifically, the average activation energies for such different kinds of irreversible structural modifications amount to 7 and 31 kJ $mol^{-1}$, respectively.[21] It was also shown that rearrangements occurring in the particle bulklike region determine a slight increase in the local volume.[21] A similar increase was not observed for rearrangements involving surface atoms, since possible excess volume created by rearrangements annihilated at the surface.

All the above mentioned evidences let some fundamental points raise. First, how could the system size actually affect the STZ activity? It can be expected, for example, that a given rearrangement could induce the operation of a neighboring potential STZ as far as the system size permits the necessary dynamics to the free volume. What could however happen when the free volume generated by local rearrangements is lost at the surface? A response to such questions could be provided by a numerical study of the mechanical behavior of nanometer-sized particles with different radius. It appears however more convenient to investigate the case of cylindrical NWs with different radial size. A compression

 

TABLE I. Values of the TB potential parameters for pure and cross interactions.

| $\alpha$-$\beta$ | $A_{\alpha\beta}$ (kJ mol$^{-1}$) | $\xi_{\alpha\beta}$ (kJ mol$^{-1}$) | $p_{\alpha\beta}$ | $q_{\alpha\beta}$ | $r_{0,\alpha\beta}$ (Å) |
|---|---|---|---|---|---|
| Ni-Ni | 13.14 | 169.40 | 10.00 | 2.70 | 2.49 |
| Ni-Zr | 20.89 | 206.35 | 8.36 | 2.23 | 2.76 |
| Zr-Zr | 15.58 | 225.74 | 9.30 | 2.10 | 3.18 |

along their axis would not in fact involve surface atoms as in the case of a spherical particle, where any local strain increase is first accommodated by rearrangements at the surface portions located along the compression axis.[21] In the case of NWs, the strain is instead more or less homogeneously distributed over the whole NW section, so that both surface and bulklike atoms are involved in any attempt to relieve exceedingly large local strains. Moreover, NWs can be virtually infinite along their axis so that size effects can be better modulated by changing only the radial size. Eventually, the statistics for STZs operating under deformation is larger for NWs than for nanometer-sized particles.

## II. NUMERICAL SIMULATIONS

Ni-Zr MGs have been often considered as the classical model systems for MGs characterized by considerable atomic size mismatch.[22] For this reason, they have been intensely investigated to shed light on both structural arrangement and dynamic behavior of atomic species.[23–27] This produced different reliable potentials[23,28–30] and a variety of data. The present work employs a semiempirical tight-binding (TB) potential based on the second-moment approximation to the electronic density of states. It has been successfully used in the past to simulate the behavior of Ni-Zr systems by MD methods[26–29] and is able to reproduce fairly well the structural and dynamical properties of pure Ni and Zr elements, as well as of their intermetallics. Numerical findings obtained from simulations focusing on the thermal diffusion of atomic species in $Ni_{50}Zr_{50}$ MGs are also in good agreement with literature data.[24,25,30,31] Similar agreement is obtained, in addition, for structural features.[30]

A $Ni_{50}Zr_{50}$ MG in bulk form was prepared starting from a random $Ni_{50}Zr_{50}$ crystalline solid solution of roughly 131 000 atoms with simple-cubic chemically disordered arrangement. The TB potential expresses the potential energy $U$ as

$$U = \sum_{i=1}^{N} \left\{ \left[ \sum_{j=1}^{N} A_{\alpha\beta} e^{-p_{\alpha\beta}(r_{ij}/r_{0,\alpha\beta}-1)} \right] - \left[ \sum_{j=1}^{N} \xi_{\alpha\beta}^{2} e^{-2q_{\alpha\beta}(r_{ij}/r_{0,\alpha\beta}-1)} \right]^{1/2} \right\}, \quad (1)$$

where $r_{ij}$ represents the distance between a pair of atoms $i$ and $j$, $r_{0,\alpha\beta}$ is the distance at 0 K of nearest neighbors (NNs) of chemical species $\alpha$ and $\beta$, and $N$ is the total number of atoms in the simulated system. Potential parameters $A_{\alpha\beta}$, $\xi_{\alpha\beta}$, $p_{\alpha\beta}$, $q_{\alpha\beta}$, and $r_{0,\alpha\beta}$ for pure and cross interactions were taken from literature[28,29] and are reported in Table I. Interactions were computed within a spherical cut-off radius $r_{cut}$ including the seventh neighbors of Zr atoms in an equilibrated hexagonal close-packed Zr lattice.

Calculations were carried out within the *NPT* ensemble with number of atoms $N$, pressure $P$, and temperature $T$ constant.[32,33] Equations of motion were solved with a fifth-order predictor-corrector algorithm[34] and a 2 fs time step. Periodic boundary conditions (PBCs) (Ref. 34) were applied along the three Cartesian directions. The initial solid solution was heated at null pressure up to 2000 K. The resulting liquid was equilibrated at 2000 K for 30 ps and successively quenched to 300 K at a rate of 2 K ps$^{-1}$. The obtained system was finally relaxed at 300 K for 50 ps. Relaxation was followed mainly by monitoring the fluctuations of kinetic and potential energies as well as of system volume. The global pair-correlation function (PCF) (Ref. 34) of the bulk, not shown for brevity, exhibits the characteristic two broad halos of amorphous structures. The relaxed MG bulk approximately occupies a $13 \times 13 \times 13$ nm$^3$ volume.

The unsupported NWs investigated in the present work were created by selecting the desired cylindrical region of radius $R$, approximately crossing the center of the relaxed bulk. The atoms inside the cylindrical region were isolated from the parent matrix by gradually canceling their interactions with the atoms outside. To this end, the $A_{\alpha\beta}$ and $\xi_{\alpha\beta}$ potential parameter values for such interactions were linearly decreased to zero in 10 ps.[35] This resulted in a satisfactory relaxation of the cylindrical free surface. It is here worth noting that the PBCs along the $z$ Cartesian direction, coincident with the NW axis, were maintained. NWs are, thus, virtually infinite along their axial direction. The radius $R$ and the size in terms of number $N$ of atoms for the different NWs considered are given in Table II.

The mechanical response of NWs to a uniaxial compression along the $z$ Cartesian direction was studied under displacement-controlled conditions. Deformation was performed in the absence of the Nosè thermostat to allow a spontaneous distribution of kinetic energy independent of any coupling with the stochastic thermal bath. A uniaxial compressive stress $\sigma_z$ operating along the NW axis was applied to obtain a constant strain rate $\dot{\varepsilon}_z$ of about $7.4 \times 10^{-2}$ ns$^{-1}$, i.e., a displacement rate of about 1 nm ns$^{-1}$. It

TABLE II. The radius $R$ and the number $N$ of atoms of the cylindrical NWs considered.

| $R$ (nm) | 1 | 2 | 3 | 4 | 5 | 6 |
|---|---|---|---|---|---|---|
| $N$ | 2381 | 9521 | 21421 | 38108 | 59532 | 85734 |

is here worth noting that such strain rate is several orders of magnitude higher than experimental ones, a condition common to all the atomistic calculations dealing with mechanical deformation of solids.[36,37] It follows that the numerical findings obtained are not immediately comparable to experimental results.[36,37] Nevertheless, numerical models are generally used to investigate the atomistic mechanisms of plastic deformation[36,37] in amorphous[15,16,37–42] and crystalline systems.[43,44] The results of these studies give in fact useful indications on the mechanical responses of real systems that could be used to address experimental research. This aspect is explained in detail once the different numerical findings have been discussed.

The mechanical responses of NWs and bulk system have been studied by evaluating the deformation curves, i.e., quantifying the stress $\sigma_z$ operating along the $z$ Cartesian direction and the corresponding strain $\varepsilon_z$. The curves were evaluated in the strain range between 0 and 0.2 to include both elastic and plastic deformation regimes.

Local atomic rearrangements were pointed out by identifying atoms exhibiting mobility in correlation with neighboring ones. The method followed is described and discussed in detail in Sec. III. The way such atoms are identified represents in fact a crucial aspect of the present work deserving a separate presentation. In addition, being the method utilized necessarily an *a posteriori* one, it must be discussed with the possibility of showing and discussing some specific results. The most accurate discussion of such methodology is, therefore, given successively. It can be anticipated here that the method employed relies on the use of specific conditions to select out all the atomic species that undergo a collective displacement, with the distance covered larger than the amplitude of a simple thermal vibration around an equilibrium position, within a given time interval $\tau$. This latter quantity, which represents a value averaged over various rearrangements, was estimated by considering the change undergone by the instantaneous potential energy of individual mobile atoms during rearrangements.

The behavior of strained NWs will be compared, whenever necessary, with the one of the initial bulk system. For this reason, the MG bulk of roughly 131 000 atoms was subjected to a uniaxial stress along the $z$ Cartesian direction at the same strain rate imposed to NWs. Also in this case, the Nosè thermostat assuring the constancy of temperature was removed during deformation. All the simulations have been carried out at least three times starting from different initial conditions to check the reliability of the obtained results.

## III. STRESS-STRAIN CURVES

The mechanical response of the investigated NWs is described by the stress-strain curves (SSCs) reported in Fig. 1, where they have been offset to avoid excessive confusion and allow a better comparison. All the systems exhibit similar behavior with easily identifiable elastic and plastic deformation stages. The elastic deformation regime gives rise to a proportional change of the stress $\sigma_z$ operating along the $z$ Cartesian direction with the strain $\varepsilon_z$. The resulting linear trend is characterized by small irregularities that increase in number and intensity in the part of SSCs related to the plastic deformation regime. For all the investigated NWs, the onset of such regime can be approximately identified by the deviation from linearity induced by the occurrence of yield phenomena. An average plateau value $\sigma_{z,p}$ is finally reached in correspondence of the plastic flow regime.

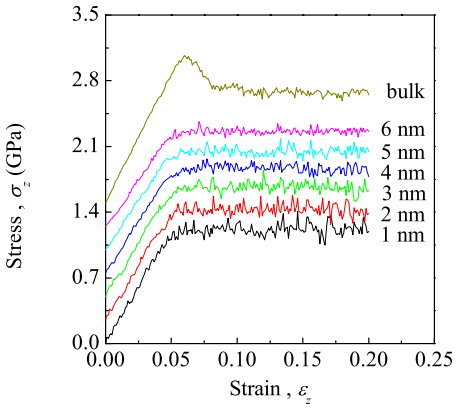


FIG. 1. (Color online) The stress $\sigma_z$ along the $z$ Cartesian direction as a function of the strain $\varepsilon_z$ for the different NWs investigated. Except for the one of the NW with radius $R$ of about 1 nm, SSCs are offset for clarity. The SSC of the bulk system is also shown for comparison.

The large bulk system shows a behavior different from the one of NWs. This clearly appears from the comparison of its SSC, also shown in Fig. 1, with the NW ones. The SSC of the bulk undergoes indeed a nonmonotonic change of slope, with the uniaxial load $\sigma_z$ reaching a maximum of about 1.5 GPa at a strain $\varepsilon_z$ of about 0.06 and then a stationary average $\sigma_{z,p}$ value of about 1.1 GPa. The mechanical response of the bulk is, however, remarkably similar to the one described in previous work[25] despite the different conditions under which the data have been obtained. The present work investigates in fact the bulk at a strain rate $\dot{\varepsilon}_z$ of about $7.4\times10^{-2}$ $\mathrm{ns}^{-1}$ and a temperature of 300 K, whereas previous work analyzes the behavior of a $Ni_{50}Zr_{50}$ MG bulk deformed at 0.13 $\mathrm{ns}^{-1}$ and at a temperature of 810 K.[25] In both cases the onset of plastic flow can be nevertheless roughly located at a strain $\varepsilon_z$ of 0.06.[25]

The average $\sigma_{z,p}$ plateau values characteristic of the plastic flow state for the different NWs considered are reported in Fig. 2 as a function of the reciprocal of the NW radius $R$, $R^{-1}$. The value pertaining to the virtually infinite bulk is also

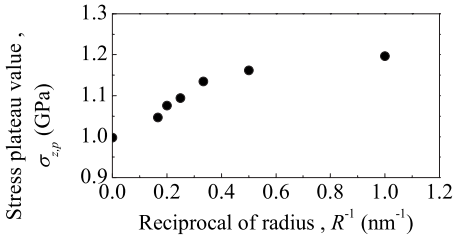


FIG. 2. The average values $\sigma_{z,p}$ of the stress $\sigma_z$ characteristic of the plastic flow state as a function of the reciprocal of the NW radius, $R^{-1}$, for the different NWs investigated. The point relative to the virtually infinite bulk system is also shown.

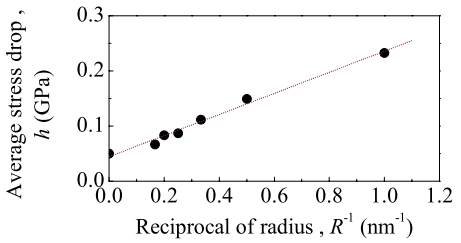


FIG. 3. (Color online) The average height $h$ of stress drops in SSCs as a function of the reciprocal of the NW radius, $R^{-1}$. The value pertaining to the virtually infinite bulk is also reported. The best-fitted line is shown.

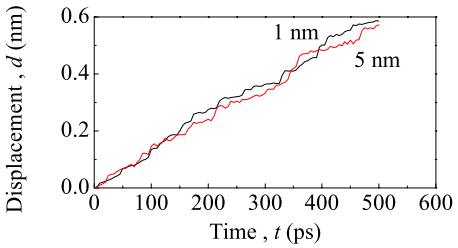


FIG. 4. (Color online) The total displacement $d$ as a function of time $t$ for the NWs with radius $R$ equal to 1 and 5 nm.

shown for comparison. It can be seen that $\sigma_{z,p}$ undergoes a slight increase as $R$ decreases. The $\sigma_{z,p}$ increase is not linear and roughly saturates at NW radii smaller than 3 nm. Smaller systems appear then to be harder than massive ones, which implies that the mechanism of plastic deformation is sensitive to the system size. In any case, the dependence of $\sigma_{z,p}$ values on the NW radius $R$ is relatively weak, with $\sigma_{z,p}$ ranging between 1 and 1.2 GPa.

Regarding these evidences, it should be noted that simple calculations indicate that the MG structure evolving in the flow state has a very low viscosity, mostly nearer to viscous fluids rather than to solid phases. Such behavior could find the rationalization already given in the literature that the viscosity drop can associated with the occurrence of a highly cooperative regime of local rearrangements.[25] The situation resembles in a sense the one expected for atoms within evolving SBs,[25] as suggested by from experimental findings.[1,2]

A further evidence of size effects in the mechanical response of $Ni_{50}Zr_{50}$ NWs to a uniaxial compression is given by the intensity of serration processes in the plastic flow state. The SSCs reported in Fig. 1 already suggest that the intensity of individual events in serrated flow is sensitive to the NW radius $R$. Correspondingly, the second part of SSCs, relatively smooth for the largest NWs, becomes increasingly irregular. A quantification of such behavior is provided by the average height $h$ of stress drops in SSCs, evaluated by averaging over all the drops observed starting from the onset of the plastic deformation regime. The $h$ values are reported in Fig. 3 as a function of the reciprocal of the NW radius $R$, $R^{-1}$. The value pertaining to the virtually infinite bulk is shown for comparison. It can be seen that $h$ increases as $R^{-1}$ increases according to an almost linear trend. Analogous inferences can be drawn by the plots shown in Fig. 4, where the total displacement $d$ is reported as a function of time $t$ for the NWs with radius $R$ equal to 1 and 5 nm. Also in these cases, the differences between the average displacement bursts in different NWs are evident.

## IV. ATOMISTIC PROCESSES

The relatively small size of the investigated systems allows the identification of the events underlying the individual displacement bursts observed during the course of the uniaxial compression. To such aim, the mobility of atomic species was monitored and the atoms classified as relatively mobile and immobile at each simulation step. Following previous work,[45] a given atom $i$ was regarded as mobile when its positions $\boldsymbol{r}_i$ at times $t$ and $t+\tau$ were able to satisfy the condition $|\boldsymbol{r}_i(t+\tau)-\boldsymbol{r}_i(t)|>0.4r_{nn}$. Here $r_{nn}$ represents the average distance of NNs indicated by the global PCF of the MG, whereas the numerical coefficient 0.4 is used to discriminate between actual atomic displacements and simple thermal vibrations.[45] Of course, the position vectors $\boldsymbol{r}_i$ take into account the displacement simply due to compression, i.e., the response of the atom $i$ in terms of affine transformation. Regarding the condition above, values slightly deviating from 0.4 do not produce significantly different results. It is also worth noting that the time period $\tau$ in the above-mentioned condition is a measure of the time interval within which the atoms move in the attempt of relieving a local strain. It can be, therefore, estimated only on *a posteriori* basis, i.e., in dependence of the system dynamics.

The aforementioned condition for identifying mobile atoms needs a further comment. As briefly stated above, the vectors $\boldsymbol{r}_i$ incorporate the information concerning the $i$th atom position change connected with the mechanical behavior of the system. This means, in turn, that the procedure adopted is similar to the one of considering the so-called deviatoric participation ratio (DPR).[8] Independent calculations show in fact that the results obtained with the aforementioned condition and with the DPR are virtually the same. The two criteria identify indeed almost the same sets of atoms. The condition here employed to systematically analyze and classify atoms has, however, the advantage of permitting the identification of mobile atoms even in the absence of deformation. It allows then the comparison between the mobility of species under exclusively thermal as well as under mechanical activation. Although not discussed in the present work for keeping the focus on the MG behavior under deformation, such comparison has been useful to better understand the role of thermal motion and local strain in triggering atomic rearrangements.

Aimed at reliably determining the time period $\tau$, the data concerning the positions $\boldsymbol{r}_i(t)$ of individual atoms $i$ were combined with the ones concerning their potential energy $u_i(t)$. This represents the total potential energy arising from the interaction of the central species $i$ with all the surrounding ones within the interatomic potential cut-off distance $r_{cut}$. Significant $u_i(t)$ increases followed by a decrease to roughly the initial value can be reasonably ascribed to atomic displacements induced by local strains. However, in some cases the dynamics of rearrangements can be masked by the con-

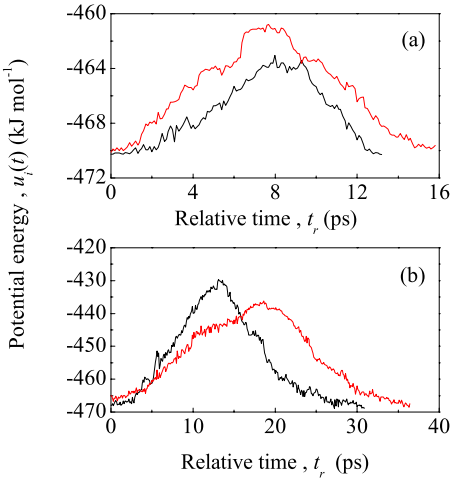


FIG. 5. (Color online) The potential energy $u_i(t)$ of individual mobile atoms $i$ as a function of the relative time $t_r$. Data concern the correlated displacement of two different atoms within larger local rearrangements involving respectively eight species located at the surface (a) and twenty-three species located in the bulk (b) of the NW system with radius $R$ of about 3 nm.

tinuous $u_i(t)$ fluctuations caused by thermal vibrations. The potential energy $u_i(t)$ of a few individual mobile atoms $i$ is reported in Figs. 5(a) and 5(b) as a function of the relative time $t_r$, which is equal to 0 roughly when the given atom $i$ starts to rearrange its position. The $u_i(t)$ curves in Fig. 5(a) belong in particular to atoms located at the surface of NWs, whereas data in Fig. 5(b) concern local rearrangements in the NW bulklike region. A systematic analysis of $u_i(t)$ curves allows us to work out the distributions $P(E_a)$ and $P(\Delta t)$ of the maximum potential energy $E_a$ and of the displacement lifetime $\Delta t$, shown in Figs. 6(a) and 6(b). $E_a$ corresponds to the maximum potential-energy value experienced by atoms during the course of their collective displacements and $\Delta t$ represents the time period over which such displacements occur. It can be seen that the $E_a$ values of $u_i(t)$ curves in Fig. 5(a) are remarkably smaller than for the $u_i(t)$ curves in Fig. 5(b). Surface rearrangements are then responsible for the

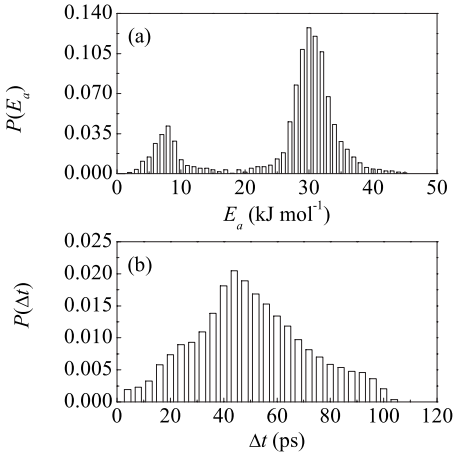


FIG. 6. The statistical distributions $P(E_a)$ of the maximum potential energy $E_a$ (a) and $P(\Delta t)$ of the displacement lifetime $\Delta t$ (b). Data refer to the case of a NW with radius $R$ of about 4 nm.

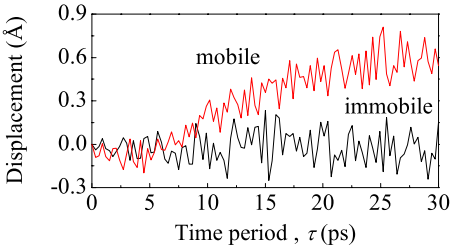


FIG. 7. (Color online) The displacements $\boldsymbol{r}_i(t+\tau)-\boldsymbol{r}_i(t)$ and $\boldsymbol{r}_j(t+\tau)-\boldsymbol{r}_j(t)$ of an atom $i$ involved in collective rearrangements (mobile) and of an atom $j$ occupying a stable position (immobile) as a function of the time period $\tau$. Data refer to bulk atoms of the NW with radius $R$ of 5 nm.

low-energy peak in the distribution $P(E_a)$ shown in Fig. 6(a), whereas bulk rearrangements are associated with the high-energy feature. Nevertheless, in both cases rearrangements take place over approximately the same time interval $\Delta t$. It can be seen that $\Delta t$ take minimum and maximum values on the order of 2 and 104 ps, respectively. The distribution $P(\Delta t)$ indicates that the most probable $\Delta t$ value is around 45 ps. The data shown in Figs. 6(a) and 6(b) refer to the case of a NW with radius $R$ of about 4 nm, but similar results are obtained in all the other cases.

The information provided by $u_i(t)$ curves was combined with the one coming from the detailed analysis of displacements $|\boldsymbol{r}_i(t+\tau)-\boldsymbol{r}_i(t)|$ of individual atoms $i$ at different $\tau$ values. The quantity $\boldsymbol{r}_i(t+\tau)-\boldsymbol{r}_i(t)$ for an atom $i$ involved in collective rearrangements is compared in Fig. 7 with the one $\boldsymbol{r}_j(t+\tau)-\boldsymbol{r}_j(t)$ for an atom $j$ occupying a stable position. Starting from a certain instant, the two relative displacements are reported as a function of the time period $\tau$. The curve belonging to the atom $j$ exhibits irregular fluctuations around a constant position, indicating the occurrence of only thermal vibrations. No significant displacement is actually observed on a time period as long as 30 ps. On the contrary, after an initial transient of about 2 ps, indicating vibrations around an approximately constant position, the atom $i$ starts a definite displacement under the influence of local strains. After about 8 ps, the behavior of the displacing atom $i$ is clearly distinguishable from simple thermal oscillations, even though the irregularities due to thermal motion temporarily increase. The data shown in Fig. 7 illustrate the average behavior of atoms displacing under the influence of local atomic strains. As a consequence, a value of time period $\tau$ equal to 10 ps permits to discriminate fairly well between displacements induced by local strains and thermal vibrations. It is on such basis that a $\tau$ value of 10 ps has been chosen to identify mobile atoms, thus, separating them from atoms vibrating around stable positions. Such $\tau$ value is nevertheless only an average value. Accordingly, by no means it is able to satisfactorily identify all the atomic displacements connected with the relief of local strains. The correct identification of mobile atoms is indeed missed in the 5% of cases. Taking into account that missed identifications concern only individual atoms, such errors introduce uncertainties of about one unit in the determination of the number of atoms undergoing a collective rearrangement. All the local rearrangements characterized by cooperative dynamics are, however, identified.

If on the one hand the physical meaning of the lifetime $\Delta t$ of cooperative rearrangements is relatively obvious, one of $E_a$ can be ascertained by studying the dynamics of displacing atoms when shearing is interrupted. The methodology applied is based on the identification of individual atoms undergoing a collective rearrangement and the evaluation of their potential energy $u_i(t)$. All the information regarding the dynamics of the sheared systems was stored to have the possibility of using each instant as a starting point of a successive simulation. Once each given mobile atom $i$ reached the maximum potential energy $E_a$, shearing was interrupted and the system left free to evolve according to its spontaneous isothermal dynamics. This was done for all the mobile atoms identified under all the different conditions and at all the simulation times. The results obtained indicate that once its potential energy $u_i(t)$ has reached the value $E_a$, the atom $i$ undergoes an irreversible rearrangement even in the absence of shearing with a probability of about 96%. The irreversible rearrangement does not involve exclusively the $i$th atom located at the top of its $u_i(t)$ curve, but also a certain number of its neighbors. The rearrangement has in fact collective character and individual atoms could not rearrange their positions without affecting the position of their neighbors. Calculations indicate in particular that any given atom neighboring the $i$th displacing one has a probability of about 50% of undergoing an irreversible displacement even though it has not reached its $E_a$ value. It should be indeed noted that the atomic species involved in a given rearrangement reach their maximum potential energy $E_a$ at slightly different instants.

The difference of probability of undergoing an irreversible displacement for atoms at the maximum potential energy and others suggests that $E_a$ is a sort of activation energy for the displacement of individual atoms. It is expected to depend on local structural features and on the nature of atomic species as well as on the strain state of the system. The average activation energy $E_a$ values for rearrangements involving bulk species, which amount to about 30 kJ $mol^{-1}$, do not agree well with a simple thermally activated diffusion scenario.[24,46] The experimental activation energy for Ni diffusion in amorphous Ni-Zr alloys amounts in fact approximately to 120 kJ $mol^{-1}$.[47] Therefore, thermally activated diffusion processes taking place in MGs in the absence of external stresses do not occur under compression. The $E_a$ values suggest instead that the observed irreversible rearrangements are more closely related to the low-energy mobility referred to in literature as low-barrier atom chain transitions.[24,47] Activation barriers of about 50 kJ $mol^{-1}$ were indeed observed in such cases.[24,47]

Based on the above observations and on the evidence that collective rearrangements occur roughly within 2 to 110 ps, it must be here stated that the irreversible cooperative rearrangements observed under shearing possess the characteristics expected for STZs. They will be, therefore, hereafter referred to as either surface or bulk STZs depending on the position of the atoms involved.

## V. PROPERTIES OF SURFACE AND BULK STZS

The obvious intrinsic difference between surface and bulk STZs is their position in the system. In the former case, irreversible rearrangements involve atomic species located at the NW cylindrical surface, whereas in the latter only bulk atoms undergo displacement. The observed different activity of surface and bulk STZs can well find explanation in the light of such characteristics. The most striking differences concern the activation energy $E_a$ of individual atom displacements, the average number of atoms participating in STZs, and their average chemical composition. All these factors are expected to be intimately correlated. The lower activation energy $E_a$ of individual atom displacements in surface STZs can be, for example, reasonably related to the smaller coordination number of surface atoms. This latter definitely affects in fact the mobility of atomic species, which generally increases as the coordination number decreases. Also the average number of atomic species involved is smaller for surface STZs than for bulk ones. The smallest surface STZ observed in the present work contained four atoms less than the smallest bulk STZ, whereas the largest surface STZ was smaller than the largest bulk STZ of twenty-two units. The average compositions of surface and bulk STZs are also significantly different. In bulk STZs Ni atoms predominate over Zr ones, with a relative content of Ni and Zr of about 0.62 and 0.38. In contrast, surface STZs exhibit an equiatomic stoichiometry.

The aforementioned characteristics of surface and bulk irreversible rearrangements can be tentatively reduced to a single conceptual framework. In the case of surface STZs, rearrangements have relatively low activation energy due to the smaller coordination number. Consequent to the low activation energy necessary to trigger the irreversible displacement, the local strain required to induce the structural change should be relatively low. In addition, the strain is not expected to affect a large number of species, i.e., to accumulate over an extended region, but rather a relatively small number of atoms. It can be then thought that almost all the atoms located in the region involved in strain accumulation are able to overcome it and undergo the collective rearrangement. Bulk STZs involve, on the contrary, atoms completely surrounded by neighbors. Under such conditions, the activation energy needed to induce irreversible rearrangements is relatively high and high is also the accumulated local strain necessary to the onset of the cooperative rearrangement. The region affected by the strain accumulation and then the number of atoms involved in the STZ operation can be, therefore, relatively large.

According to the activation energy $E_a$ values and to the qualitative observations above, the most severe local strain conditions allowing for collective rearrangements to take place are required by bulk STZs. Under such circumstances, it is reasonable to think that STZ activity should preferably involve the most mobile species, i.e., the ones that can more easily undergo a displacement. In the present case, such species are represented by Ni atoms. Ni atoms behave indeed as fast diffusers in Zr.[23–25,47] The larger number of Ni atoms involved in bulk STZs with respect to Zr ones can be therefore regarded as the condition determining the lowest activation barrier. In other words, at any given level of local strain Ni atoms are expected to be more responsive than Zr ones. Such mobility difference between Ni and Zr species is expected to become particularly evident at relatively high strain

levels. This is the case of bulk STZs, the activation of which requires in fact large strains. The case of surface STZs is clearly different. Only relatively low strains are necessary to trigger the irreversible rearrangement. At such low strain levels, the difference in mobility of Ni and Zr species is not significant and surface STZs involve, thus, approximately the same number of Ni and Zr atoms, mirroring the stoichiometry of the $Ni_{50}Zr_{50}$ MG system investigated.

The approximate conceptual framework briefly sketched above suggested pursuing the research in two different directions concerning, respectively, the role of atomic volume and the occurrence of particular STZ activity when rearrangements involve both surface and bulklike atoms. The former point arises from the evidence that atomic volumes are related to the mobility of atomic species in either individual or collective displacements in the absence of strain and are also generally expected to play a role under deformation conditions. Regarding the latter point, it should be noted that unusual features can emerge in STZ activity when no clear distinction between surface and bulk STZs can be made. Such kind of local irreversible rearrangements are observed in particular in NWs with radius $R$ smaller than 4 nm, their occurrence becoming increasingly probable as the NW radius $R$ decreases. The case of STZs involving both surface and bulk atoms was then specifically studied.

## VI. ATOMIC VOLUME AND BULK STZ ACTIVITY

The evaluation of the atomic volume $\Omega_i$ of each $i$th atom requires first a reliable distinction between surface and bulk species. It is indeed only for these latter that the atomic volume can be evaluated. Taking advantage of the obvious difference between surface and bulk atoms, surface species were identified on the basis of their coordination number, which is smaller than for bulk species. To such aim, it is worth noting that $Ni_{50}Zr_{50}$ MGs contain Ni and Zr species with coordination numbers significantly different from each other and from the equilibrium values characteristic of their crystalline lattices. In particular, Ni atoms can exhibit coordination numbers as small as 7, whereas Zr atoms can be even 12-fold coordinated. These numbers agree remarkably well with MD literature on $Ni_{50}Zr_{50}$ MGs.[30,31] Based on these evidences, Ni and Zr atoms were regarded as surface species whenever their coordination numbers were smaller than 7 and 12, respectively. A further check was carried out on their position. This was characterized in terms of radial distance from the NW axis in order to ascertain that they are in a cylindrical layer about one atom thick at the NW surface. Once surface and bulk atoms were identified, the atomic volume $\Omega$ of these latter species was estimated by performing a Voronoi space tessellation.[48]

Attention was in particular focused on the properties of mobile atoms. Possible volume effects in the mechanical response of NWs in both elastic and plastic deformation stages preceding the flow state were, thus, characterized. The volume $\Omega_i$ of each $i$th mobile atom was evaluated and the average volume of bulk species participating in STZs calculated. The average initial volume $\bar{\Omega}_{in}$ of atoms involved in bulk STZs, i.e., the volume before the STZ operation, amounts approximately to $1.03 \pm 0.05\ \bar{\Omega}$, where $\bar{\Omega}$ represents the average volume of the species in the considered system. The average final volume $\bar{\Omega}_{fin}$, i.e., the volume immediately after the STZ operation, is instead roughly equal to $1.06 \pm 0.05\ \bar{\Omega}$. Irreversible rearrangements in STZs, therefore, produce a local volume increase of about $0.03\ \bar{\Omega}$. Such average volume increase points out that the STZ activity should produce a dilatation of the system volume as a function of the time. A rough calculation of the total volume dilatation per time unit can be easily done by considering the distribution $P(n_{STZ})$ of the size $n_{STZ}$ of bulk STZs, which corresponds to the number of atoms involved in a given bulk STZ. $P(n_{STZ})$ is reported in Fig. 8 as a function of $n_{STZ}$ for the NW with radius $R$ of about 5 nm. Similar distributions are obtained for the NWs with radius $R$ equal to about 3, 4, and 6 nm. The distribution has an approximately Gaussian shape, with the average around a $n_{STZ}$ value of 27 atoms. At each STZ operation the system volume increases then of about $1.2 \times 10^{-5}\ \bar{\Omega}$. Being the average frequency of STZ operation roughly equal to 19 $ns^{-1}$, the rate of volume dilatation amounts to about $2.4 \times 10^{-4}\ \bar{\Omega}\ ns^{-1}$. Such value approximately corresponds to $7 \times 10^{-23}\ m^3\ s^{-1}$, which is exceedingly small to be detectable in experiments.

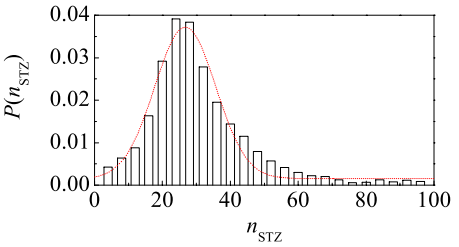


FIG. 8. (Color online) The statistical distribution $P(n_{STZ})$ of the STZ size $n_{STZ}$. The best-fitted Gaussian function is also shown. Data refer to the NW with radius $R$ of about 5 nm.

It must be, however, noted that the excess volume locally generated by the operation of bulk STZs is soon redistributed among the atomic species surrounding the STZ. The dispersion of the excess atomic volume cannot be followed in detail due to the thermal fluctuations of atoms, which prevent the quantification of the smallest local volume fluctuations. However, in the largest NWs considered STZ activity is often observed in the neighborhood of a given STZ once it has operated. From this point of view, the behavior of relatively large NWs is, therefore, similar to the one of bulk systems.

## VII. POSSIBLE CORRELATION BETWEEN SUCCESSIVE STZS

The possible relationship between different STZs operating consecutively in large bulk systems is quite difficult to investigate. Various STZs operate indeed almost simultaneously in different positions, which seriously hinders any attempt of pointing out causal relationships between them. The situation is, however, remarkably simpler in small systems such as the NWs considered in the present work. Under the hypothesis that STZs are uniformly distributed in the

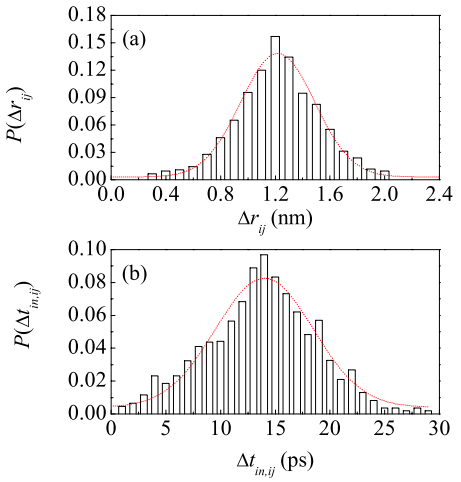


FIG. 9. (Color online) (a) The statistical distribution $P(\Delta r_{ij})$ of the distance $\Delta r_{ij}$ between any given $i$th STZ and the successive $j$th one. (b) The statistical distribution $P(\Delta t_{in,ij})$ of the time interval $\Delta t_{in,ij}$ separating the onset of two successive STZs. Data refer in both cases to the NW with radius $R$ of about 6 nm. Best-fitted Gaussian functions are also shown.

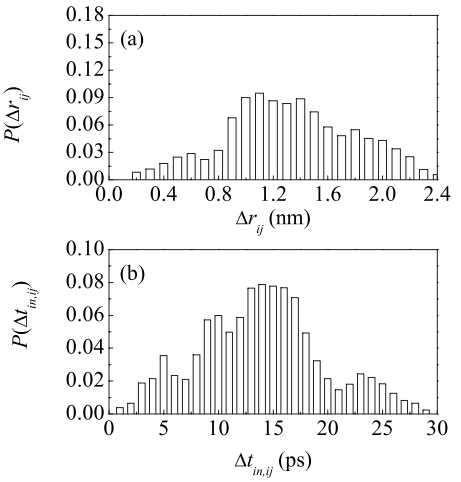


FIG. 10. (a) The statistical distribution $P(\Delta r_{ij})$ of the distance $\Delta r_{ij}$ between any given $i$th STZ and the successive $j$th one. (b) The statistical distribution $P(\Delta t_{in,ij})$ of the time interval $\Delta t_{in,ij}$ separating the onset of two successive STZs. Data refer in both cases to the NW with radius $R$ of about 3 nm.

system, the smaller volume acts here as a limiting factor for their activation frequency, being dependent on the total number of potential STZs in the system volume. It becomes then possible to monitor in greater detail the occurrence of local rearrangements and to analyze their possible correlation. Such analysis must be necessarily based on combined time and distance criteria. In fact, almost all the different regions of a glassy system can be in principle involved in local rearrangements on relatively long time scales. A distance criterion alone cannot be, therefore, sufficient to ascertain the correlation of neighboring STZs.

The case of the NW with radius $R$ of about 6 nm was studied first. The STZ activity was followed by identifying the atomic species involved and determining the position $\boldsymbol{r}_{cm}$ of the center of mass (CM) of the STZ as well as the time $t_{in}$ at which the STZ operation approximately initiates. The quantity $\boldsymbol{r}_{cm}$ represents a sort of average STZ position and provides a rough tool to compare the positions of different STZs. The evaluation of the time $t_{in}$ allows, analogously, comparing the times at which different STZs operate. Attention was focused only on the first STZ operating after any given one. To such aim, the distance $\Delta r_{ij}$ between any given $i$th STZ and the immediately successive $j$th one was evaluated. It corresponds to the difference $|\boldsymbol{r}_{cm,i}-\boldsymbol{r}_{cm,j}|$ between the positions of the CMs of the STZs considered. The statistical distribution $P(\Delta r_{ij})$ of $\Delta r_{ij}$ is reported in Fig. 9(a). The statistical distribution $P(\Delta t_{in,ij})$ of the time interval $\Delta t_{in,ij}$ separating the onset of two successive STZs is instead shown in Fig. 9(b). $\Delta t_{in,ij}$ corresponds to the difference $t_{in,i}-t_{in,j}$ between the times at which two successive STZs $i$ and $j$ initiate. It can be seen that in both Figs. 9(a) and 9(b) data arrange according to an approximately Gaussian curve. The most probable distance $\Delta r_{ij}$ between successive bulk STZs amounts roughly to 1.2 nm, which indicates that the local irreversible rearrangements are remarkably close. The $P(\Delta t_{in,ij})$ peak occurs furthermore at about 14 ps, indicating that also the time interval $\Delta t_{in,ij}$ between successive events is remarkably short.

Both the aforementioned evidences can be considered as a clue to the correlation of successive STZs in the bulk of the NW with radius $R$ equal to about 6 nm. The behavior of the NWs is, however, sensitive to the radius $R$. This can be easily inferred by the statistical distributions $P(\Delta r_{ij})$ and $P(\Delta t_{in,ij})$ of the different NWs investigated. The $P(\Delta r_{ij})$ and $P(\Delta t_{in,ij})$ for the NW with radius $R$ of about 3 nm are reported in Figs. 10(a) and 10(b) for sake of illustration. These curves are characterized by a larger number of peaks, with no definite predominant feature at a distance $\Delta r_{ij}$ of 1 to 1.2 nm or at time intervals $\Delta t_{in,ij}$ of 10 to 18 ps. This suggests that the degree of correlation between consecutive STZs can significantly change as the NW radius $R$ decreases. In general, a progressive modification of the shape of statistical distributions $P(\Delta r_{ij})$ and $P(\Delta t_{in,ij})$ with $R$ is observed. Distributions broaden and, also due to the smaller number of STZs observed, exhibit increasingly multimodal features.

An idea of the modification of the system behavior with the NW radius is given by the $\eta$ data reported in Fig. 11 as a function of $R$. The quantity $\eta$ is equal to the average of the product between the $\Delta r_{ij}$ and $\Delta t_{in,ij}$ values for any two consecutive STZs. Intuitively, a small $\eta$ value indicates relatively small average $\Delta r_{ij}$ and $\Delta t_{in,ij}$ values, whereas a large $\eta$

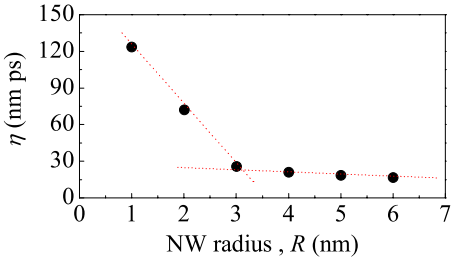


FIG. 11. (Color online) The $\eta$ quantity as a function of the NW radius $R$. Dotted lines are a guide to the eyes.

value indicates relatively large average $\Delta r_{ij}$ and $\Delta t_{in,ij}$ values. The points in Fig. 11 show that $\eta$ increases as $R$ decreases. It appears that STZs occur on the average at larger distances and separated by longer time intervals as the NW size decreases. Despite the poor statistics and the small number of points prevent definite conclusions, data seem to arrange according to two approximately linear trends with different slope. The change of slope roughly occurs at a $R$ value of 3 nm, which is also the $R$ value above which the number of STZs involving both bulk and surface species significantly increases.

A few additional words of comment concerning the statistical distributions $P(\Delta r_{ij})$ and $P(\Delta t_{in,ij})$ are here necessary. First, it is worth remembering that the results discussed above and the ones that will be dealt with hereafter regard the behavior of NWs and of the bulk system under elastic deformation conditions and at the beginning of the plastic regime. By no means the numerical findings described before and in the following must be intended as referred to the flow state. The latter originates from the cooperation of a number of STZs activated by relatively high local strains due to the large plastic deformation. Its study does not permit thus to easily identify the critical conditions allowing for a potential STZ to operate. Less drastic strain conditions are necessary to such aim. Furthermore, no significant difference between the behavior of STZs under elastic and plastic deformation conditions is observed. The STZ activity exhibits of course a higher degree of complexity as the average strain $\varepsilon_z$ increases. This is, however, ascribable to the increased number of STZs operating and to their autocatalytic behavior, which remarkably complicates the analysis of the system dynamics. Different is the case of STZs operating under the flow state regime. It is not discussed here for brevity and, more important, for keeping the study focused on the identification of STZs under suitable conditions favoring a progress in the rationalization of their activity. Nevertheless, it can be reported that the degree of cooperativeness exhibited by mobile atoms displacing in the flow state regime is much higher than under elastic deformation conditions and at the beginning of the plastic regime. The case of the bulk can be instructive. In a sense, almost the whole system becomes soon involved in a collective behavior characterized by the contemporary displacement of a very large number of atoms. Such features are in principle compatible with what is believed to occur within a SB. The whole system could even be regarded as a SB. It is, however, worth noting that the relatively small size of the bulk system does not allow to infer whether the observed behavior can be really interpreted in terms of SBs or not. In the case of NWs, the flow state behavior can also determine the fracture of the system, with two relatively large portions displacing with respect to each other along an inclined average plane.

Coming back to the behavior of STZs in NWs, in the light of the above mentioned evidences it is tempting to connect the observed behavior with the different properties of STZs involving exclusively bulk atoms and both bulk and surface species. Aimed at investigating the activity of the latter kind of STZs, the localized rearrangements taking place in the NW with radius $R$ of about 1 nm were monitored in detail. In this case, all the STZ events observed involve both bulk and surface atoms. An immediately evident difference with the case of the NW with radius $R$ of about 6 nm is the fact that successive STZs are distributed essentially at random along the NW axis. No evidence of correlation between consecutive rearrangements was obtained, being these also separated by apparently random time intervals. The atoms involved in two successive STZs separated by a time interval about 45 ps long are shown in Fig. 12(a). It can be seen that the two STZs are approximately 4 nm distant along the NW axis. For comparison, two correlated STZs in the NW with radius of about 6 nm are shown in Fig. 12(b). This permits to immediately see the difference between the two cases, with the nearest atoms of the correlated STZs distant less than 0.6 nm. In accordance with the observations above, the distributions $P(\Delta r_{ij})$ and $P(\Delta t_{in,ij})$ for the NW with radius $R$ of about 1 nm tend to be uniform, with no significant feature resembling a peak indicating more probable values.

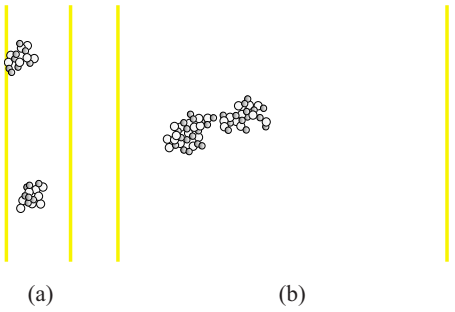


FIG. 12. (Color online) (a) Two successive STZs separated by a time interval about 45 ps long and approximately 4 nm distant along the axis of the NW with radius $R$ of about 1 nm. (b) Two correlated STZs separated by a time interval about 8 ps long and approximately 0.6 nm distant along the axis of the NW with radius $R$ of about 6 nm. Ni and Zr atoms are in dark and light gray, respectively. Vertical lines indicate the NW profile.

The behavior of NWs with radii of about 1 and 6 nm was further investigated by identifying in the 6 nm NW all the bulk STZs followed by a neighboring surface STZ. The bulk STZs occurring after a surface STZ were also identified. The CM positions of the bulk STZ, of the consecutive surface STZ and of the successive bulk STZ were then compared. It appears that the apparent correlation between the initial bulk STZ and the successive surface STZ is lost when this latter and the successive bulk STZ are considered. Neither positions nor time intervals suggest a possible correlation. In fact, whereas the surface STZ takes place always in the neighborhood of the preceding bulk STZ, the STZ occurring after the surface one can actually be located everywhere in the system. Analogous observations concern the time intervals between STZs. The occurrence of a surface STZ determines thus a loss of correlation in a given chain of consecutive STZs. The above mentioned evidences indicate then that the involvement of surface atoms significantly modifies the behavior of potential STZs.

In the attempt of clarifying at least in part these aspects, attention was again focused on the atomic volume of bulk species involved in STZs in the case of the NW with radius $R$ of about 1 nm. Following the previously described procedure, the volume $\Omega_i$ of each $i$th mobile atom was estimated

and the average volume $\bar{\Omega}$ of bulk atoms involved in each STZ operation calculated. It is perhaps worth remembering that surface species are excluded by such calculation being impossible to define for them a volume analogous to the one defined for bulk species. The average initial volume $\bar{\Omega}_{in}$ of species involved in STZs before their operation amounts approximately to $1.02 \pm 0.03$ $\bar{\Omega}$, a value similar to the one already computed for bulk species. The average final volume $\bar{\Omega}_{fin}$ attained immediately after the STZ operation is instead roughly equal to $0.90 \pm 0.04$ $\bar{\Omega}$. In the light of the behavior of bulk STZs in relatively large NWs, this latter result is quite surprising. It points out that, in contrast with the average volume increase of about 0.03 $\bar{\Omega}$ undergone by bulk STZs, an average volume decrease of about $-0.12$ $\bar{\Omega}$ takes place when STZs involve both bulk and surface species. It follows that the activity of STZs involving both bulk and surface species determines a loss of free volume.

The behavior observed in the different cases, including the one concerning the bulk system, can be tentatively rationalized by the dynamics of free volume. In the first place, the loss of free volume at the surface apparently explains why two consecutive STZs involving both bulk and surface species are uncorrelated. In fact, under the hypothesis that free volume facilitates localized atomic rearrangements, local losses of free volume somewhat hinder the operation of other STZs in the neighborhood. The sequence of STZs observed is therefore decided exclusively by criteria of local structural stability in connection with the local strain level attained, i.e., the most unstable STZ operates first. In the second place, the operation of bulk STZs can be explained by resorting to both local structural instability and free volume migration. The excess free volume generated by a given bulk STZ can indeed migrate and concur to define the stability level of a neighboring local arrangement of atoms. If a potential STZ is relatively close to an operated bulk STZ, it is possible that the excess free volume generated by the latter could favor the rearrangement of the former in response to external stress solicitations. It follows that the migration of free volume can be regarded as a sort of relatively short-ranged interaction process between an operated bulk STZ and a neighboring potential STZ. In the third place, the generation of excess free volume consequent to the activity of bulk STZs is in principle able to explain their autocatalytic behavior and their capability of generating a SB. The operation of STZs is indeed expected to become more and more facilitated as the local free volume increases, being the generation of excess free volume in a given bulk region to determine a local avalanche of STZs. Finally, the mechanistic scenario based on the migration of free volume allows a satisfactory rationalization of the size dependence of the mechanical properties of MGs. It appears indeed that the systems deviate from the behavior of a bulk not only as a consequence of the smaller number of STZs due to the smaller volume available, but also as a consequence of the increase in the number of STZs involving both bulk and surface species. It is under such conditions that STZs apparently loose their autocatalytic ability. A sort of hardening can be therefore expected in deformed nanometer-sized MGs.

The whole body of numerical findings and inferences above discussed, and in particular the loss of free volume at the surface when suitable STZ activity occurs, suggests a few experimental scenarios for the possible exploration of the aforementioned free volume effects. The most obvious, but also most difficult, one concerns the direct investigation of the mechanical response of NWs. Operating with the necessary accuracy it could be possible to point out the signature of free volume dynamics in the SSCs characteristic of NWs when compared to the SSCs of massive systems. The greater difficulty is however represented by the capability of synthesizing NWs with amorphous structure. A second appealing scenario could be the one dealing with the mechanical response of highly porous systems, with the MG scaffold having characteristic size on the order of nanometers. Here a synthetic route could be the one of transforming an initially massive system into a highly porous one, which could be then submitted to mechanical tests. The porosity should assure a very large surface area and then favor the loss of free volume even during elastic deformation conditions. It follows that a progressive hardening of the material should be observed.

Finally, it is worth noting that the whole interpretation of the free volume effects is based on the accurate quantification of its value and of the error bars associated. The method employed in the present investigation, i.e., the quantification of the average atomic volumes defined by a Voronoi polyhedra space tessellation, is relatively well suited to such aim. As far as the investigated systems are well relaxed, it has good sensitivity and permits to follow the dynamics of free volume. Uncertainties increase, of course, as the temperature increases. Various troubles can be then envisaged when analyses concern extended plastic deformation and flow state regimes, where local temperature rise can be expected and actually as a consequence of the rapid cooperative rearrangement of a number of atoms. This is another reason for which dealing with the flow state regime has been avoided and simulations have been performed at 300 K. The method employed is nevertheless quite robust and allows the identification of very small atomic volume differences, as clearly shown by the application of the same algorithms to the case of crystalline systems with different content of lattice defects of various nature.

## VIII. CONCLUSIONS

The numerical findings obtained from MD simulations indicate that the mechanical response to uniaxial compression of MG NWs is remarkably different from the one of a corresponding bulk system. In both cases, the deformation process is mediated by the operation of consecutive STZs. Correspondingly, local atomic structures rearrange in the attempt of relieving the local strains accumulated as a consequence of the applied stress. The behavior of STZs involving exclusively bulk atoms is the same in NWs and bulks. However, NWs also exhibit the operation of STZs involving both bulk and surface atoms as well as only surface atoms. This latter kind of STZs does not seem to significantly determine the NW behavior. Local atomic rearrangements at the surface

only involve a relatively small number of species and the size effect has simply a geometrical character, the number of surface STZs being proportional to the number of surface atoms. Much more interesting in view of a comparison between NWs and bulk systems are instead the STZs in which both bulk and surface atoms are involved. Their number scales nontrivially with the NW size and, in addition, they significantly affect the degree of correlation between consecutive STZs. Their overall size effect is, therefore, a combination of at least two factors.

In such respect, the fundamental evidence is represented by the loss of correlation between consecutive STZs originated by the system size decrease. The STZs operating in bulk systems or in relatively large NWs, such as the one with radius of about 6 nm, exhibit a considerable degree of correlation. Once a given STZ has occurred, the probability of observing a consecutive STZ in the neighborhood within relatively short times is quite high. Such probability decreases with the system size and consecutive STZs become almost completely uncorrelated in the NW with radius of about 1 nm. The reason for such behavior apparently lies in the dynamics of free volume in the different systems investigated. Regarding these aspects, the present study can be considered only as a preliminary one. A richer statistics is in fact necessary to draw sound conclusions from the details of STZ operation.

Nevertheless, the results obtained suggest that the system size can significantly affect the dynamics of free volume within the system. Calculations indicate that excess free volume is generated by the operation of STZs involving only bulk atoms. Under the hypothesis that the operation of a potential STZ becomes more and more probable with the local increase in free volume, the migration of the free volume generated by an operated STZ can in principle trigger the operation of neighboring STZs. However, STZs involving both bulk and surface atoms do not produce excess free volume. On the contrary, free volume is lost at the surface. As a consequence, whenever an operated bulk STZ activates a STZ involving surface species, the degree of correlation with successive ones is lost. This is the case of the smallest NWs considered, for which the STZ activity essentially consists of the operation of STZs involving both bulk and surface species.

Although new light has been thrown on the atomistic mechanisms of deformation of nanometer-sized MGs, further work is necessary to adequately address all the questions raised by the results here discussed. For example, what happens to nanometer-sized MG systems when all the excess free volume is lost? Can such a loss determine a crystallization? Which is the minimum free volume of a MG? Finding a response to such questions could require considerable computational resources and relatively long times, but could as well assure significant progress in the field.

## ACKNOWLEDGMENTS

Financial support has been given by the University of Cagliari. A. Ermini, ExtraInformatica s.r.l. is gratefully acknowledged for his kind assistance and technical support.

*delogu@dicm.unica.it

[1] C. A. Schuh, T. C. Hufnagel, and U. Ramamurty, Acta Mater. **55**, 4067 (2007).
[2] MRS Bull. **32**, issue 8 (2007).
[3] A. S. Argon and H. Y. Kuo, Mater. Sci. Eng. **39**, 101 (1979).
[4] A. S. Argon, J. Phys. Chem. Solids **43**, 945 (1982).
[5] V. V. Bulatov and A. S. Argon, Modell. Simul. Mater. Sci. Eng. **2**, 167 (1994).
[6] V. V. Bulatov and A. S. Argon, Modell. Simul. Mater. Sci. Eng. **2**, 185 (1994).
[7] V. V. Bulatov and A. S. Argon, Modell. Simul. Mater. Sci. Eng. **2**, 203 (1994).
[8] M. L. Falk and J. S. Langer, Phys. Rev. E **57**, 7192 (1998).
[9] M. L. Falk, Phys. Rev. B **60**, 7062 (1999).
[10] J. S. Langer, Phys. Rev. E **64**, 011504 (2001).
[11] A. Lemaitre, Phys. Rev. Lett. **89**, 195503 (2002).
[12] A. Inoue, W. Zhang, T. Tsurui, A. R. Yavari, and A. L. Greer, Philos. Mag. Lett. **85**, 221 (2005).
[13] H. Bei, S. Xie, and E. P. George, Phys. Rev. Lett. **96**, 105503 (2006).
[14] J. S. Langer, Scr. Mater. **54**, 375 (2006).
[15] Y. Shi and M. L. Falk, Phys. Rev. Lett. **95**, 095502 (2005).
[16] Y. Shi, M. B. Katz, H. Li, and M. L. Falk, Phys. Rev. Lett. **98**, 185505 (2007).
[17] Q. Zheng, S. Cheng, J. H. Strader, E. Ma, and J. Xu, Scr. Mater. **56**, 161 (2007).
[18] A. Donohue, F. Spaepen, R. C. Hoagland, and A. Misra, Appl. Phys. Lett. **91**, 241905 (2007).
[19] H. Guo, P. F. Yan, Y. B. Wang, Z. F. Zhang, J. Tan, M. L. Sui, and E. Ma, Nature Mater. **6**, 735 (2007).
[20] Z. W. Shan, J. Li, Y. Q. Cheng, A. M. Minor, S. A. Syed Asif, O. L. Warren, and E. Ma, Phys. Rev. B **77**, 155419 (2008).
[21] F. Delogu, Phys. Rev. B **77**, 174104 (2008).
[22] in *Physical Metallurgy*, 4th ed., edited by R. W. Cahn and P. Haasen (North-Holland, Oxford, 1996).
[23] I. Ladadwa and H. Teichler, Phys. Rev. E **73**, 031501 (2006).
[24] H. Teichler, J. Non-Cryst. Solids **293-295**, 339 (2001).
[25] K. Brinkmann and H. Teichler, Phys. Rev. B **66**, 184205 (2002).
[26] C. Massobrio, V. Pontikis, and G. Martin, Phys. Rev. B **41**, 10486 (1990).
[27] P. Mura, P. Demontis, G. B. Suffritti, V. Rosato, and M. Vittori Antisari, Phys. Rev. B **50**, 2850 (1994).
[28] C. Massobrio, V. Pontikis, and G. Martin, Phys. Rev. Lett. **62**, 1142 (1989).
[29] F. Cleri and V. Rosato, Phys. Rev. B **48**, 22 (1993).
[30] Ch. Hausleitner and J. Hafner, Phys. Rev. B **45**, 115 (1992).
[31] Ch. Hausleitner and J. Hafner, Phys. Rev. B **45**, 128 (1992).
[32] H. C. Andersen, J. Chem. Phys. **72**, 2384 (1980).
[33] S. Nosè, J. Chem. Phys. **81**, 511 (1984).
[34] M. P. Allen and D. Tildesley, *Computer Simulations of Liquids*

(Clarendon Press, Oxford, 1987).
[35] F. Delogu, Phys. Rev. B **72**, 205418 (2005).
[36] M. F. Horstemeyer, M. I. Baskes, and S. J. Plimpton, Acta Mater. **49**, 4363 (2001).
[37] R. G. Hoagland and M. I. Baskes, Scr. Mater. **39**, 417 (1998).
[38] Q.-K. Li and M. Li, Appl. Phys. Lett. **88**, 241903 (2006).
[39] Y. Shi and M. L. Falk, Phys. Rev. B **73**, 214201 (2006).
[40] N. P. Bailey, J. Schiotz, A. Lemaitre, and K. W. Jacobsen, Phys. Rev. Lett. **98**, 095501 (2007).
[41] E. A. Jagla, Phys. Rev. E **76**, 046119 (2007).
[42] M. L. Manning, J. S. Langer, and J. M. Carlson, Phys. Rev. E **76**, 056106 (2007).
[43] E. Rabkin, H.-S. Nam, and D. J. Srolovitz, Acta Mater. **55**, 2085 (2007).
[44] L. A. Zepeda-Ruiz, B. Sadigh, J. Biener, A. M. Hodge, and A. V. Hamza, Appl. Phys. Lett. **91**, 101907 (2007).
[45] H. Zhang, D. J. Srolovitz, J. F. Douglas, and J. A. Warren, Phys. Rev. B **74**, 115404 (2006).
[46] C. Donati, J. F. Douglas, W. Kob, S. J. Plimpton, P. H. Poole, and S. C. Glotzer, Phys. Rev. Lett. **80**, 2338 (1998).
[47] F. Faupel, W. Frank, M.-P. Macht, H. Mehrer, V. Naundorf, K. Rätzke, H. R. Schober, S. K. Sharma, and H. Teichler, Rev. Mod. Phys. **75**, 237 (2003).
[48] J. L. Finney, Proc. R. Soc. London, Ser. A **319**, 495 (1970).